Separation Science and Technology

Publication details, including instructions for authors and subscription information:
http://www.informaworld.com/smpp/title~content=t713708471

Theory of Clarifier Operation. V. A Simplified Model, Design Aspects, and Time-Dependent Feeds

David J. Wilson[a]; Elaine C. Graves[a]; KARL B. Schnelle JR.[a]
[a] DEPARTMENTS OF CHEMISTRY AND OF ENVIRONMENTAL AND WATER, RESOURCES ENGINEERING VANDERBILT UNIVERSITY NASHVILLE, TENNESSEE

To cite this Article Wilson, David J. , Graves, Elaine C. and Schnelle JR., KARL B.(1980) 'Theory of Clarifier Operation. V. A Simplified Model, Design Aspects, and Time-Dependent Feeds', Separation Science and Technology, 15: 7, 1429 — 1443
To link to this Article: DOI: 10.1080/01496398008056095
URL: http://dx.doi.org/10.1080/01496398008056095

SEPARATION SCIENCE AND TECHNOLOGY, 15(7), pp. 1429–1443, 1980

Theory of Clarifier Operation. V. A Simplified Model, Design Aspects, and Time-Dependent Feeds

DAVID J. WILSON,* ELAINE C. GRAVES, and KARL B. SCHNELLE, JR.

DEPARTMENTS OF CHEMISTRY AND OF ENVIRONMENTAL AND WATER RESOURCES ENGINEERING
VANDERBILT UNIVERSITY
NASHVILLE, TENNESSEE 37235

Abstract

Simplified mathematical models for slurry settling under quiescent conditions and in two types of upflow clarifier are presented. Effective floc radius and a coefficient in the expression for the viscosity, the only adjustable parameters, are determined by fitting to published data on settling velocities of stirred ferric hydroxide flocs. These parameters are then used to calculate rates of sludge blanket rise in a reactor-clarifier operated at various flow rates. Agreement with data on ferric hydroxide flocs is satisfactory. The responses of clarifiers of two different designs to transient hydraulic overloads are then calculated. The models indicate that the reactor-clarifier (fed in the middle, sludge wasted at the bottom) performs better than a clarifier which is fed at the bottom and from the middle of which sludge is wasted.

INTRODUCTION

We earlier proposed a theoretical model for quiescent settling and settling in clarifiers (*1–4*) which was tested experimentally on suspensions of ferric hydroxide (*5, 6*). The relevant theory is reviewed in the first reference. We found that reasonable values of the model parameters permitted the theory to calculate quiescent settling velocities in good agreement with experiment over a range of 0.03 to 0.35 in settleable solids volume fraction (SSVF), and that these parameters adequately described the behavior of premixed ferric hydroxide slurries in an upflow clarifier when the parameters were used in a mathematical model for the operation

*To whom correspondence should be addressed.

of the device. It was found that several of the parameters did not affect the observable results to any extent. This was fortunate, because it would have been quite difficult to assign *a priori* values to these quantities.

Our mathematical models were quite elaborate, and included a rather detailed representation of floc coagulation and disruption. As a result, the computer programs were fairly large, substantial quantities of computer memory were required, and running times were long. These factors limit the use of the models for design purposes, which require variation of a good many floc and apparatus parameters to determine the optimum clarifier to be used in a given situation. This motivated our attempt to develop a simplified model for settling; this should eliminate the parameters which do not significantly affect clarifier performance, and should have much reduced memory and computer time requirements. These constraints dictate the elimination of a detailed mechanism for floc coagulation and disruption. There follows the construction of such a simplified model, its testing against quiescent settling data for $Fe(OH)_3$, and its use in the investigation of the effects of variations in clarifier geometry and of time-dependent influent flow rates and compositions.

ANALYSIS

We derive in detail the equations governing the operation of the upflow sludge blanket clarifier diagrammed in Fig. 1. This device is fed at the bottom, sludge is wasted from a horizontal plane somewhere in the middle, and effluent is discharged at the top. Then we present the equations for another type of clarifier which is fed in the middle, and from the bottom of which sludge is wasted, as shown in Fig. 2. To avoid the computational

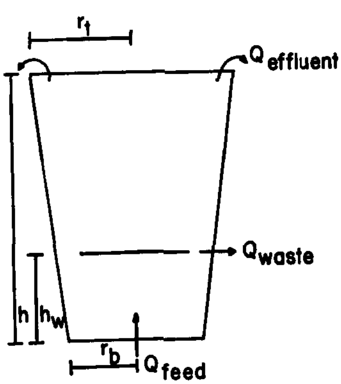

FIG. 1. An upflow sludge blanket clarifier.

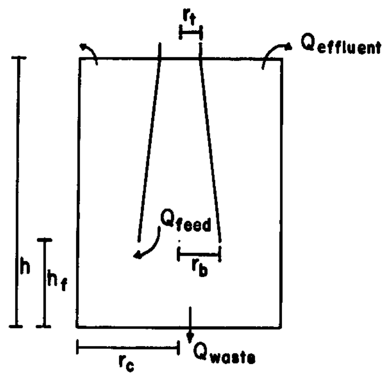

FIG. 2. A reactor-clarifier of the type used by Graves.

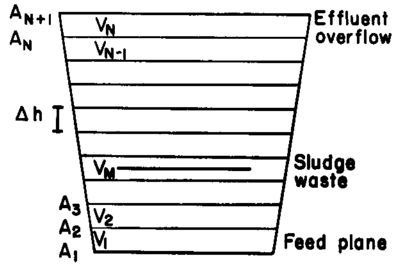

FIG. 3. Partitioning of the upflow sludge blanket clarifier into slabs for numerical integration of the conservation equations.

burden inherent in any theory which includes flocculation, we consider a monodisperse nonflocculating precipitate.

The clarifier is partitioned into N horizontal slabs, as shown in Fig. 3. Notation is as follows.

r_t = radius of the top of the clarifier
r_b = radius of the bottom of the clarifier
h = height of the clarifier
h_w = height of the sludge wasting plane
V_n = volume of slab n
A_n = area of the bottom of slab n and of the top of slab $n - 1$
Δh = slab thickness
M = index of slab containing the sludge wasting plane
N = number of horizontal slabs into which the clarifier is partitioned, and the index of the top slab
Q_{feed} = volumetric feed rate

Q_{waste} = volumetric sludge wasting rate
$Q_{\text{effluent}} = Q_{\text{feed}} - Q_{\text{waste}}$
$c_0(t)$ = influent solids volume fraction
ρ_s = density of precipitate
ρ_l = density of water
η_0 = viscosity of water
η = viscosity of slurry
r = radius of a precipitate particle
u = |velocity| of a particle relative to the surrounding liquid
v_n^u = velocity of a particle at the top of the nth slab relative to the laboratory (+ if particle is rising)
v_n^l = velocity of a particle at the bottom of the nth slab relative to the laboratory
$c_n(t)$ = settleable solids volume fraction in the nth slab at time t

The volume of the nth slab is given by

$$V_n = \frac{\pi}{3}\left(\frac{r_t - r_b}{h}\right)^2\left[\left(n\Delta h + \frac{r_b h}{r_t - r_b}\right)^3 - \left((n-1)\Delta h + \frac{r_b h}{r_t - r_b}\right)^3\right] \quad (1)$$

The area of the bottom of the nth slab is

$$A_n = \pi\left[r_b + (n-1)\Delta h\,\frac{r_t - r_b}{h}\right]^2 \quad (2)$$

The influent volumetric feed rate and influent concentration we assume are given by

$$\begin{aligned} Q_{\text{feed}} &= Q_1, \quad t_1 > t \text{ or } t_2 < t \quad (3)\\ &= Q_2, \quad t_1 \le t \le t_2 \\ c_0 &= c_{01}, \quad t_1 > t \text{ or } t_2 < t \quad (4)\\ &= c_{02}, \quad t_1 \le t \le t_2 \end{aligned}$$

which permits us to investigate the effects of transient hydraulic or solids overloads on clarifier performance.

In the interests of simplicity, we replace the rather elaborate formula for the viscosity of the slurry which we previously used (*7*) by a simple exponential containing one adjustable parameter, α:

$$\eta = \eta_0 \exp(\alpha c) \quad (5)$$

This permits us to calculate the |velocity| of a particle with respect to the surrounding liquid by recursive use of Eq. (6). (See Ref. *8*.)

$$u(c) = \frac{2g(\Delta\rho)r^2}{9\eta}\left[1 + \frac{1}{4}\left(\frac{\rho_{sl} r u}{2\eta}\right)^{1/2} + \frac{0.34\rho_{sl} r u}{12n}\right]^{-1} \quad (6)$$

where $g = 980\ \mathrm{cm/sec^2}$

$\Delta\rho = \rho_s - \rho_{sl}$

$\rho_{sl} = \rho_s c + \rho_l(1 - c)$ = density of slurry

c = volume fraction solids

The velocities of the particles with respect to the laboratory are then given by

$$v_n{}^l = \frac{Q_{\text{feed}}}{A_n} - u(c_{n-1})(1 - c_{n-1}), \qquad n = 2, \ldots, M \tag{7}$$

$$= \frac{Q_{\text{feed}} - Q_{\text{waste}}}{A_n} - u(c_{n-1})(1 - c_{n-1}), \qquad n = M + 1, \ldots, N \tag{8}$$

$$v_n{}^u = \frac{Q_{\text{feed}}}{A_n + 1} - u(c_n)(1 - c_n) \tag{9}$$

$$= \frac{Q_{\text{feed}} - Q_{\text{waste}}}{A_n + 1} - u(c_n)(1 - c_n), \qquad n = M, \ldots, N \tag{10}$$

We then write out material balance equations for the various slabs, which yields the following results. In these equations $S(v)$ is a unit step function such that

$$S(v) = 0, \qquad v \leq 0$$
$$= 1, \qquad v > 0$$

$$\frac{dc_1}{dt} = [-A_2\{S(v_1{}^u)v_1{}^u c_1 + S(-v_2{}^l)v_2{}^l c_2\} + Q_{\text{feed}}c_0]/V_1 \tag{11}$$

$$\frac{dc_M}{dt} = [A_M\{S(v_{M-1}^u)v_{M-1}^u c_{M-1} + S(-v_M{}^l)v_M{}^l c_M\} - A_{M+1}\{S(v_M{}^u)v_M{}^u c_M + S(-v_{M+1}^l)v_{M+1}^l c_{M+1}\} - Q_{\text{waste}}c_M]/V_M \tag{12}$$

$$\frac{dc_N}{dt} = [A_N\{S(v_{N-1}^u)v_{N-1}^u c_{N-1} + S(-v_N{}^l)v_N{}^l c_N\} - A_{N+1}S(v_N{}^u)v_N{}^u c_N]/V_N \tag{13}$$

$$\frac{dc_n}{dt} = [A_n\{S(v_{n-1}^u)v_{n-1}^u c_{n-1} + S(-v_n{}^l)v_n{}^l c_n\} - A_{n+1}\{S(v_n{}^u)v_n{}^u c_n + S(-v_{n+1}^l)v_{n+1}^l c_{n+1}\}]/V_n,$$
$$n = 2, \ldots, M - 1, M + 1, \ldots, N - 1 \tag{14}$$

These equations are then integrated forward in time by means of a standard predictor-corrector formula (*9*), which starts as follows:

predictor:

$$c_n^*(\Delta t) = c_n(0) + \Delta t \frac{dc_n}{dt}(0) \tag{15}$$

corrector:

$$c_n(\Delta t) = c_n(0) + \frac{\Delta t}{2}\left[\frac{dc_n}{dt}(0) + \frac{dc_n^*}{dt}(\Delta t)\right] \tag{16}$$

The general algorithm is

predictor:

$$c_n^*(t + \Delta t) = c_n(t - \Delta t) + 2\Delta t \frac{dc_n}{dt}(t) \tag{17}$$

corrector:

$$c_n(t + \Delta t) = c_n(t) + \frac{\Delta t}{2}\left[\frac{dc_n}{dt}(t) + \frac{dc_n^*}{dt}(t + \Delta t)\right] \tag{18}$$

One can then obtain the solids distribution in the clarifier at any time. The sludge solids volume fraction (SSVF) is then given by

$$\begin{aligned} \text{SSVF} = \{&c_{M-1}S(v_{M-1}^u)v_{M-1}^u A_M + c_M[S(-v_M{}^l)v_M{}^l A_M - S(v_M{}^u)v_M{}^u A_{M+1}] \\ &- c_{M+1}[S(-v_{M+1}^l v_{M+1}^l A_{M+1})]\}/Q_{\text{waste}} \end{aligned} \tag{19}$$

The effluent solids volume fraction (ESVF) is given by

$$\text{ESVF} = c_N v_N{}^u S(v_N{}^u) A_{N+1}/(Q_{\text{effluent}}) \tag{20}$$

The influent solids flux (ISF) is given by

$$\text{ISF} = c_0 Q_{\text{feed}} \tag{21}$$

The sludge solids flux (SSF) is

$$\text{SSF} = \text{SSVF} \cdot Q_{\text{waste}} \tag{22}$$

The effluent solids flux (ESF) is given by

$$\text{ESF} = \text{ESVF} \cdot (Q_{\text{effluent}}) \tag{23}$$

The percent solids removal as estimated from the sludge composition (SRSC) is given by

$$\text{SRSC} = 100\text{SSF}/\text{ISF} \tag{24}$$

The percent solids removal as estimated from the effluent composition (SREC) is

$$\text{SREC} = 100[1 - (\text{ESF}/\text{ISF})] \tag{25}$$

The position of the top of the sludge blanket as a function of time is a matter of some interest. If the model is being operated with $r_t = r_b$ and $Q_{feed} = Q_{waste} = 0$ and the clarifier initially filled with slurry, this information can be used to obtain theoretical quiescent settling velocities which can be matched to experimental settling velocity vs solids concentration curves to obtain values for r (effective particle radius) and α (coefficient in the expression for the slurry viscosity). If the model is being operated on a general case, movements of the top of the sludge blanket can yield information on the impacts of time-dependent influent concentrations and feed rates. We estimate the height of the top of the sludge blanket as follows. Find that value of n, m, for which

$$c_m \geq \frac{c_0}{2} \qquad \text{and} \qquad c_{m+1} < \frac{c_0}{2} \tag{26}$$

Then calculate blanket height h_b by linear interpolation as

$$h_b = (m - 1/2)\Delta h + \Delta h \, \frac{(c_m - c_0/2)}{c_m - c_{m+1}} \tag{27}$$

This gives the blanket height at any time t. The velocity of the top of the sludge blanket, v_b, was then calculated from

$$v_b = \frac{h_b(n_2\Delta t) - h_b(n_1\Delta t)}{(n_2 - n_1)\Delta t} \tag{28}$$

We next examine the modifications necessary to model the clarifier diagrammed in Fig. 2. Changes in notation are as follows.

r_c = radius of clarifier shell
r_b = radius of bottom of inner cone
r_t = radius of top of inner cone
h = height of clarifier, $= N\Delta h$
h_f = height of feed plane, $= M\Delta h$
M = index of the slab containing the feed plane

The area of the bottom of the nth slab is given by

$$\begin{aligned} A_n &= \pi r_c^2, \qquad 1 \leq n \leq M \\ &= \pi(r_c^2 - R_n^2), \qquad M + 1 \leq n \leq N \end{aligned} \tag{29}$$

where

$$R_n = r_t + (r_b - r_t)\left(\frac{N + 1 - n}{N - M}\right) \tag{30}$$

The volume of the nth slab is given by

$$V_n = \pi r_c^{\,2}\Delta h, \qquad 1 \le n \le M$$
$$= \pi\left[r_c^{\,2} - \frac{1}{3}(R_n^{\,2} + R_nR_{n+1} + R_{n+1}^2)\right]\Delta h, \quad M + 1 \le n \le N \qquad (31)$$

The velocities of the particles with respect to the laboratory are given by

$$v_n^{\,l} = -\frac{Q_{\text{waste}}}{A_n} - u(c_{n-1})(1 - c_{n-1}), \qquad n = 2, \dots, M \qquad (32)$$

$$= \frac{Q_{\text{feed}} - Q_{\text{waste}}}{A_n} - u(c_{n-1})(1 - c_{n-1}), \qquad n = M + 1, \dots, N \qquad (33)$$

$$v_n^{\,u} = -\frac{Q_{\text{waste}}}{A_{n+1}} - u(c_n)(1 - c_n), \qquad n = 1, \dots, M - 1 \qquad (34)$$

$$= \frac{Q_{\text{feed}} - Q_{\text{waste}}}{A_{n+1}} - u(c_n)(1 - c_n), \qquad n = M, \dots, N \qquad (35)$$

where $u(c)$ is given by Eq. (6).

The material balance equations for the individual slabs are as follows.

$$\frac{dc_1}{dt} = [-A_2\{S(v_1^{\,n})v_1^{\,n}c_1 + S(-v_2^{\,l})v_2^{\,l}c_2\} - Q_{\text{waste}}c_1]/V_1 \qquad (36)$$

$$\frac{dc_M}{dt} = [A_M\{S(v_{M-1}^u)v_{M-1}^u c_{M-1} + S(-v_M^{\,l})v_M^{\,l}c_M\}$$
$$- A_{M+1}\{S(v_M^{\,u})v_M^{\,u}c_M + S(-v_{M+1}^l)v_{M+1}^l c_{M+1}\} + Q_{\text{feed}}c_0]/V_M \qquad (37)$$

$$\frac{dc_N}{dt} = [A_N\{S(v_M^{\,u}{}_{-1})v_N^{\,n}{}_{-1}c_{N-1} + S(-v_N^{\,l})v_N^{\,l}c_N\} - A_{N+1}S(v_N^{\,u})v_N^{\,u}c_N]/V_N \qquad (38)$$

$$\frac{dc_n}{dt} = [A_n\{S(v_n^{\,u}{}_{-1})v_{n-1}^u c_{n-1} + S(-v_n^{\,l})v_n^{\,l}c_n\}$$
$$- A_{n+1}\{S(v_n^{\,u})v_n^{\,u}c_n + S(-v_{n+1}^l)v_{n+1}^l c_{n+1}\}]/V_n,$$
$$n = 2, \dots, M - 1, M + 1, \dots, N - 1 \qquad (39)$$

These equations can then be integrated by the predictor-corrector method.

The sludge solids volume fraction is given by

$$\text{SSVF} = c_1 \qquad (40)$$

and the effluent solids volume fraction by Eq. (20). ISF, SSF, ESF, SRSC, and SREC are given by Eqs. (21)–(25).

RESULTS

Before the model can be used, we must assign values to the parameters describing the floc. The theory contains three such parameters: the floc density ρ_s, the floc particle effective radius r, and the coefficient α in Eq. (5) for the slurry viscosity. We attempt to fit the model to Graves' data on stirred ferric hydroxide flocs (*5*, *6*). We accept her calculation of ρ_s from the density of geothite (FeOOH) and the volume of settled floc produced; she estimated $\rho_s = 1.0079$ g/cm^3 relative to $\rho_l = 1.0000$ g/cm^3. This leaves us with two parameters, r and α, to be chosen. We select r to yield quiescent settling velocities at low solids concentration ($c_0 = 0.05$) in agreement with experiment. Then we select α to yield quiescent settling velocities at high solids concentration ($c_0 = 0.30$) in agreement with experiment. The quiescent settling velocity at low c_0 is relatively insensitive to α but quite sensitive to r, while the quiescent settling velocity at relatively large c_0 is strongly dependent on both α and r. Convergence to a satisfactory fit is rapid; we started with $r = 0.025$ cm and $\alpha = 10$, and four pairs of runs (at $c_0 = 0.05$ and 0.30) led to the results shown in Fig. 4. The curves bracket Graves' data for stirred $Fe(OH)_3$ flocs precipitated from ferric sulfate with NaOH or $Ca(OH)_2$ at pH 6 or 10. The points are computed quiescent settling velocities obtained with the values of r and α indicated. The fit is slightly better than we obtained with our earlier, much more elaborate model, which lends support to the choice of the simple exponential dependence of slurry viscosity on volume fraction solids.

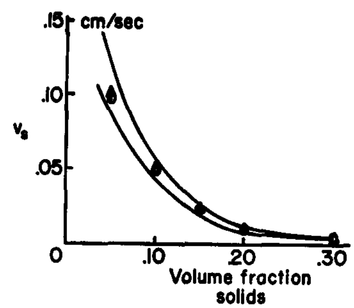

FIG. 4. Fit of the simple theory to Graves' quiescent settling velocity data. The two solid curves bracket her data on the settling of stirred $Fe(OH)_3$ flocs prepared from $Fe_2(SO_4)_3$ and $Ca(OH)_2$ or NaOH at pH's of 6 and 10. (▲) Theoretical quiescent settling velocities with $\alpha = 13.0$, $r = 0.037$ cm, $\rho_s = 1.0079$ g/cm^3, ρ_l 1.0000 g/cm^3, $h = 30$ cm, $r_t = r_b = 10$ cm, $N = 30$, $Q_{feed} = Q_{waste} = 0$, $\eta_0 = 0.01$ poise. (●) Theoretical quiescent settling velocities with $\alpha = 12.0$, $r = 0.035$ cm, other parameters as above.

Figures 5–8 show the time dependence of the solids distributions in the quiescent settling simulations. At low solids concentrations the slurry–supernate interface is found to be more diffuse than at high solids concentrations, as was observed by Graves (5). The model also roughly simulates slow compaction at the bottom of the column, as shown particularly clearly in Fig. 5 and also in Fig. 9, in which the height of the slurry–supernate interface is plotted as a function of time for various initial concentrations of solids.

Graves determined the rate of rise or fall of the top of the sludge blanket

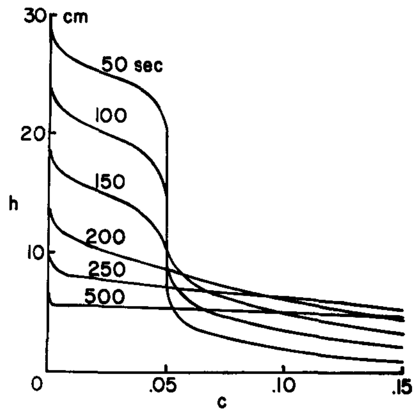

FIG. 5. Quiescent settling profiles at various times during settling. $\alpha = 13.0$, $r = 0.037$ cm, $\rho_s = 1.0079$ g/cm^3, $\rho_l = 1.0000$ g/cm^3, $h = 30$ cm, $r_t = r_b = 10$ cm, $N = 30$, $Q_{feed} = Q_{waste} = 0$, $\eta_0 = 0.01$ poise, $c_0 = 0.05$.

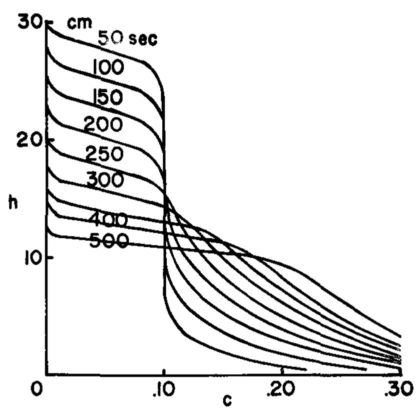

FIG. 6. Quiescent settling profiles at various times during settling. $c_0 = 0.10$, other parameters as in Fig. 5.

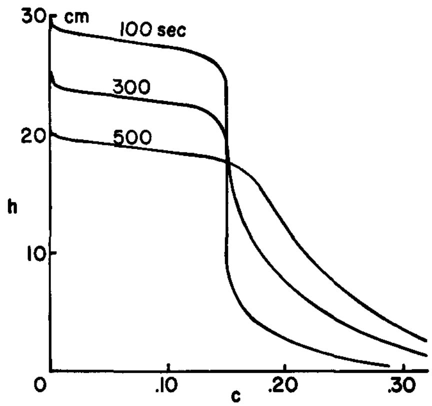

FIG. 7. Quiescent settling profiles at various times during settling. $c_0 = 0.15$, other parameters as in Fig. 5.

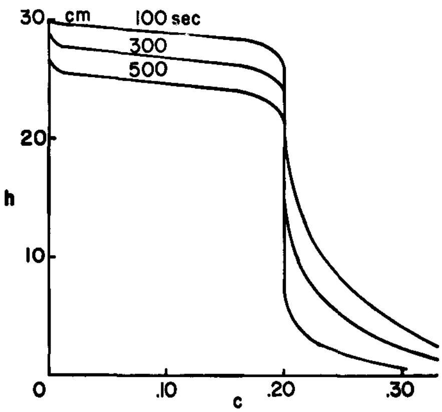

FIG. 8. Quiescent settling profiles at various times during settling. $c_0 = 0.20$, other parameters as in Fig. 5.

in an upflow clarifier of the type diagrammed in Fig. 2. She used ferric hydroxide flocs prepared by the same procedure as was used for making the flocs used in the quiescent settling tests. In Fig. 10 her experimental results are compared with our calculated rates of blanket rise. We used the parameters found to fit the quiescent settling data and the physical dimensions of her clarifier in these calculations. The agreement is reasonably good except at $Q_{\text{feed}} = 126.7$ cm/sec, at which the experimental point appears to be out of line with both the calculated point and the other experimental points.

Volumetric flow rates to clarifiers frequently show large variations with

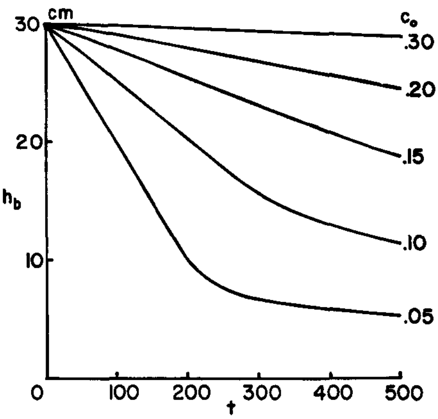

FIG. 9. Position of the top of the sludge blanket during quiescent settling as a function of time. c_0 as indicated, other parameters as in Fig. 5.

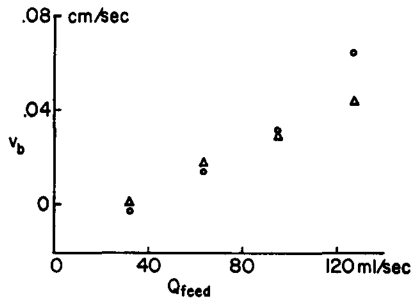

FIG. 10. Plot of blanket rise velocity as a function of Q_{feed} in Graves' reactor-clarifier. $r_c = 22.6, r_t = 5.1,\ r_b = 12.7,\ h = 121.9, h_{feed} = 30.5$ cm, $Q_{waste} = 0$, other parameters as in Fig. 5.

time. If the duration and flow rate of such a slug are not too large, the clarifier may well be able to cope with it without excessive discharge of solids even if a steady-state analysis indicates that the clarifier would be overloaded at the flow rate of the slug. The upper portion of the clarifier (that volume between the top of the sludge blanket and the top of the clarifier) acts as a buffer to permit the clarifier to absorb shock loads. This is illustrated in Fig. 11, in which the clarifier's ability to deal with overloads of various magnitudes and 1000 sec duration is examined. In these runs the sludge waste flow rate was held constant. The dimensions of the clarifier and the floc characteristics were those pertaining to Graves' clarifier and well-mixed ferric hydroxide. One can approximately estimate the time interval τ during which the clarifier can tolerate an overload feed

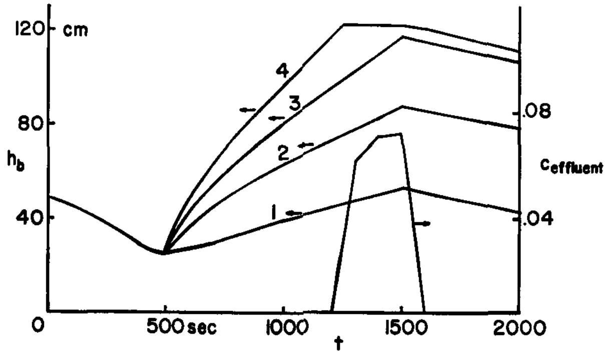

FIG. 11. Effect of shock hydraulic loadings on a reactor-clarifier. The height of the sludge blanket is plotted as a function of time for the clarifier described in Fig. 10. $t_1 = 500$ sec, $t_2 = 1500$ sec, $c_0 = 0.10$; $Q(t < t_1$ or $t > t_2) = 50$ cm^3/sec; $Q(t_1 < t_2) = 100, 150, 200$, and 250 cm^3/sec (Curves 1 through 4, respectively). $Q_{waste} = 20$ cm^3/sec, other parameters as in Fig. 10.

rate Q'_{feed}; it is given by

$$\frac{h - h_b(0)}{v_b(Q'_{feed})} = \tau \tag{41}$$

where $h_b(0)$ is the position of the top of the sludge blanket at the start of the overload, $v_b(Q'_{feed})$ is the rise velocity of the top of the blanket for a feed rate Q'_{feed}, and h is the height of the clarifier. We assume that Q_{waste} is being held constant.

The slopes of the plots of $h_b(t)$ between $t = 1500$ and 2000 sec (after the feed rate has dropped back to its "normal" value) give us a measure of the rate at which the clarifier recovers from the slug of influent. The more rapidly the plots decrease with increasing t in this region, the more quickly does the clarifier recover and become able to accept another slug without a high probability of solids escaping in the effluent. The capacity of a clarifier to treat a slug of influent and the rate of its recovery require models capable of handling time-dependent feeds. At the highest flow rate ($Q_{feed} = 250$ mL/sec, the biggest slug), solids break through into the effluent. This is shown in Fig. 11. The area under the curve ESVF is proportional to the mass of solids discharged in the effluent during the slug,

$$\begin{aligned} M_{effluent} &= \int (Q_{feed} - Q_{waste})\mathrm{ESVF}(t)\,dt \\ &= (Q'_{feed} - Q_{waste}) \int \mathrm{ESVF}(t)\,dt \end{aligned} \tag{42}$$

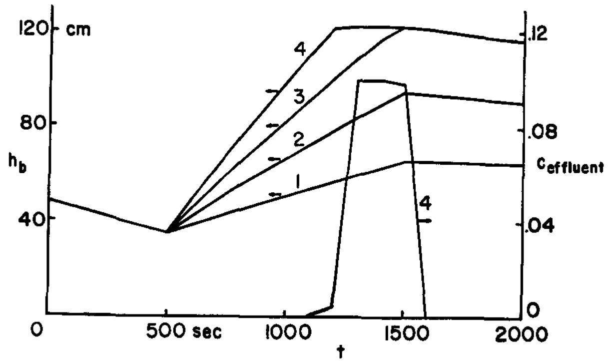

FIG. 12. Effect of shock hydraulic loadings on an upflow sludge blanket clarifier. The height of the sludge blanket is plotted as a function of time for a clarifier of the type sketched in Fig. 1, and the overall dimensions are identical to those of the reactor-clarifier described in Figs. 10 and 11. $r_t = r_b = 22.6$, $h = 121.9$, $h_{\text{waste}} = 30.5$ cm, $Q_{\text{waste}} = 20\ \text{cm}^3/\text{sec}$, other parameters as in Figs. 5 and 10.

if solids are discharged in the effluent only during the period of excessive flow rate.

In Fig. 12 we see plots of $h_b(t)$ for a clarifier of the type illustrated in Fig. 1. The dimensions of this clarifier are identical to those of the clarifier modeled to yield the data shown in Fig. 11, except that the inner cone is absent, influent is delivered to the bottom of the clarifier, and sludge is discharged at a height of 30.5 cm. This clarifier was simulated with exactly the same floc and flow rates as the clarifier of Fig. 11. The "normal" flow rate was taken as 50 mL/sec, and 1000-sec slugs of 100, 150, 200, and 250 mL/sec were applied between $t = 500$ and 1500 sec. This clarifier does not perform as well as the reactor-clarifier. Its rate of recovery after receiving an overload is roughly half as fast as that of the reactor-clarifier, and the largest overload pulse causes it to discharge about 37% more solids in the effluent than does the reactor-clarifier.

Each of the runs plotted in Figs. 11 and 12 required about 170 sec of time on an XDS Sigma 7 computer. The model is evidently sufficiently frugal of computer time to permit its use for routine design calculations.

Acknowledgment

We are indebted for a grant from the Vanderbilt University Research Council in support of this work.

REFERENCES

1. J. H. Clarke, A. N. Clarke, and D. J. Wilson, *Sep. Sci. Technol.*, *13*, 767 (1978).
2. D. J. Wilson, *Ibid.*, *13*, 881 (1978).
3. A. N. Clarke, D. J. Wilson, and J. H. Clarke, *Ibid.*, *13*, 895 (1978).
4. D. J. Wilson, A. N. Clarke, and R. H. French, *Ibid.*, *14*, 1 (1979).
5. E. C. Graves, K. B. Schnelle, Jr., and D. J. Wilson, *Ibid.*, *14*, 923 (1979).
6. E. C. Graves, Ph.D. Dissertation, Vanderbilt University, 1979.
7. V. Vand, *Phys. Colloid Chem.*, *52*, 277 (1948).
8. G. M. Fair, J. C. Geyer, and D. A. Okun, *Water and Wastewater Engineering, Vol. II. Wastewater Treatment and Disposal*, Wiley, New York, 1968, Section 25–2.
9. L. G. Kelly, *Handbook of Numerical Methods and Applications*, Addison-Wesley, Reading, Massachusetts, 1967, p. 186.

Received by editor January 21, 1980